THOMAS JEFFERSON NATIONAL ACCELERATOR FACILITY
12000 Jefferson Avenue
Newport News, VA 23606

JLAB-TN-21-024

Tech Note Number:
MEG0002021-R003 Rev-

TITLE: ELECTROMAGNETIC DESIGN OF MQW MAGNET FOR THE CEBAF 200 keV INJECTOR BEAMLINE

BY: Seetha-Lakshmi Lalitha

DATE: 05 /20 /2021

Approver: Joe Grames

-	The initial release	05/20/2021
REV.	DESCRIPTION	DATE
SUMMARY OF CHANGES FROM PREVIOUS REVISION:		

Approved: 08/11/2021; E-Sign ID: 445894; Signed By: Reviewer 1: J. Grames; Reviewer 2: J. Grames; DCG Quality Check: T.

Contents

Electromagnetic Design Report of MQW Magnet in the CEBAF 200 keV Injector Beamline

1 Introduction

This document describes (a) the design and analysis of the new MQW type, air-core quadrupole corrector magnet in the CEBAF 200 keV injector beamline [1], (b) coil manufacturing requirements and magnet assembly details, (c) the quality check procedure of the production coils and magnetic test plan, and (d) performance validation by the electromagnetic (EM) simulation of the models with the actual dimensions for the coils and the support structure for the magnet assembly. This magnet is required to compensate for the astigmatic focusing introduced by the Wein filters.

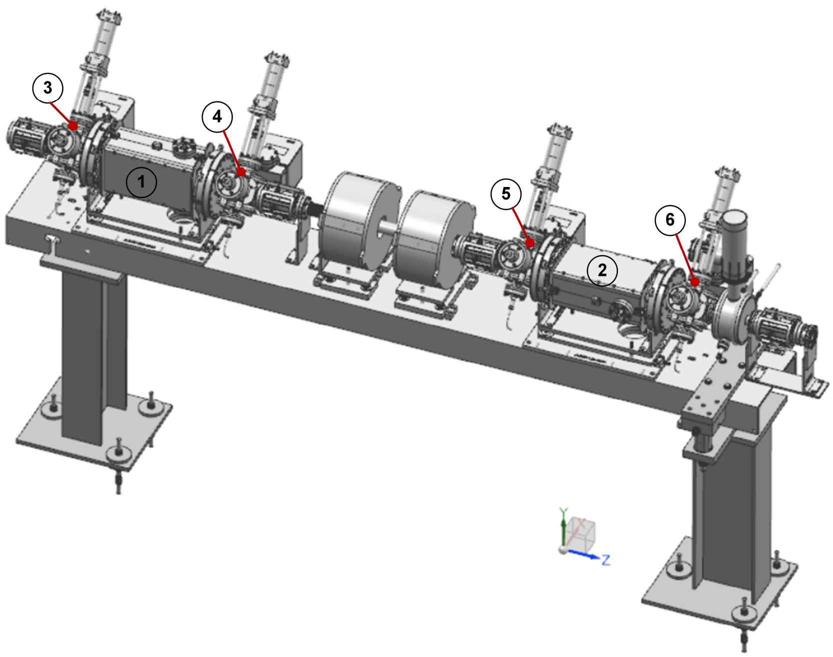

Figure 1: Schematic of the Wien filter girder assembly in the 200 keV injector beamline [2]. Labels 1 and 2 denote respectively the vertical and horizontal Wien filter. The labels 3, 4, 5, and 6 points respectively to the four of the new MQW type quadrupole magnets, MQW1I03, MQW1I04, MQW1I05, and MQW1I06. The beam direction is from the left to right side of this page (i.e along +Z direction as shown in the figure).

The MQW replaces the existing skew dipole corrector coil assembly in the beamline. Among the four of these new magnets in the Wien girder assembly (see Figure 1), MQW1I03 (label 3) and MQW1I04 (label 4) are situated upstream and downstream of the vertical Wien Filter, MWFI104 (label 1). Similarly, MQW1I05 (label 5) and MQW1I06 (label 6) are associated with the succeeding horizontal Wien filter, MWF1I06 (label 2).

2 Design Requirements

2.1 The new MQW type magnet to place adjacent to the vertical or horizontal Wein filter shall be identical in design and performance.

2.2 The magnet coils shall fit on a CF six-way cross assembly which also shares connections to the vacuum and beam diagnostic components in the girder assembly (see inset of Figure 2).

2.3 The permissible space, length-wise for the magnet assembly shall remain the same as that for its predecessor in the 100 keV beamline.

2.4 The magnet shall provide a maximum integrated field gradient of 0.01 T (100 Gauss). The specified radius (R_{GFR}) of the good field region (GFR) is 7.5 mm.

2.5 The magnet polarity settings, fringe field limits, and magnetic homogeneity requirements are not specified for the new magnet design.

2.6 All components used in the magnet assembly shall withstand a maximum of 200°C to comply with the bake-out procedure for the beamline vacuum components.

3 Design Approach

The design parameters were set according to the magnet functional specification, and the mechanical and system-level integration requirements listed in section 2 of this document. The new three-dimensional (3D) electromagnetic (EM) model was developed through an iterative design engineering analysis and using the Siemens NX CAD software package (Ver.12). The model is presented in Cartesian coordinates with the positive Z-axis (longitudinal axis) pointing in the beam direction, the Y-axis along the vertical direction, and the X-axis pointing radially outwards. The origin of the reference coordinate system coincides with the magnet center.

The 3D EM calculations were performed with the ANSYS Maxwell (Version: 2020 R2) software. The ANSYS Workbench package (Version: 2020 R2) was used for relevant multi-physics analysis to support the development of the coil and bobbin model as well as the magnet mounting structure around the CF vacuum cross assembly. The conductor parameters and coil manufacturing aspects were appropriately integrated into the design.

The main results are the magnetic field characteristics, Lorentz force, resistance, inductance, and stored energy of the magnet. The multipole field calculations at R_{GFR} of 7.5 mm were carried out by the Fourier decomposition of the simulated field map at selected values of coil excitation currents in the range of interest. The main parameters are extracted from the radial field component of the quadrupole and higher-order field harmonics. The effective magnetic length (L_{eff}) of the quadrupole magnet and the deviation of integrated quadrupole field uniformity at R_{GFR} $\left(\sum_{n^*} B'_{r,n^*}\,(R_{GFR}, z)\right)$ are given as follows:

$$L_{eff} = \frac{\int_{z=-0.3m}^{z=+0.3m} B_{r,n=2}(R_{GFR},\ z)\,.\,dz}{B_{r,n=2}(R_{GFR},\ z=0)} \qquad (1)$$

The term in the numerator of equ.1 represents the value of the integrated strength of the leading quadrupole radial field component at R_{GFR} over the z range of ± 0.3 m from the magnet center ($z = 0$). The term in the denominator is the strength of the corresponding field component at the magnet center.

$$\sum_{n^*} B'_{n^*}\,(R_{GFR}, z) = \sum_{n^*} \frac{\int_{z=-0.3m}^{z=+0.3m} B_{r,n^*}(R_{GFR},\ z)\,.\,dz}{\int_{z=-0.3m}^{z=+0.3m} B_{r,n=2}(R_{GFR},\ z)\,.\,dz} \qquad (2)$$

where $B_{r,n^*}(r = R_{GFR}, z)$ refers to the value of the allowed higher-order multipole radial field component at R_{GFR} for any given position z along the longitudinal axis of the magnet. The number n^* denotes the order of the multipole field errors.

The reported quadrupole integrated field quality (%) is

$$QIFQ\ (\%) = \left(1 - \sum_{n^*} B'_{r,n^*}\,(R_{GFR}, z)\right) * 100 \qquad (3)$$

The coil resistance at 20 C is calculated using the copper resistivity of 1.724×10^{-8} Ω.m.

The final 3D NX model derived from this design analysis forms the basis for the CAD drawings (see Table 2) used to manufacture the parts and the assembly of the magnet.

4 Magnetic Design Description

4.1 The preliminary design studies suggest that the flat racetrack geometry for coils offers a compact magnet that fulfills the functional requirements. Figure 2 shows the MQW magnet mounted on the stainless-steel CF six-way vacuum cross-fitting. The four coils (QC1, QC2, QC3, and QC4) are arranged in the normal quadrupole geometry around the longitudinal tubing of the 6-way cross-assembly such that the distance between the bottom side of the opposite pair of coils is 76 mm. The four coil-bobbin assemblages are held in place by suitably sized two mount frames mechanically fastened to the top flange of the bobbin. The mount frames are positioned symmetrically on the opposite side of the respective CF cross tubing as shown in the figure. The bottom surface of the bobbin flange is shaped appropriately to eliminate the mechanical interference from the outside surface of the upstream and downstream CF flanges on the six-way cross-assembly. The dimensions of the coils and major components for the magnet assembly are given in Table 1.

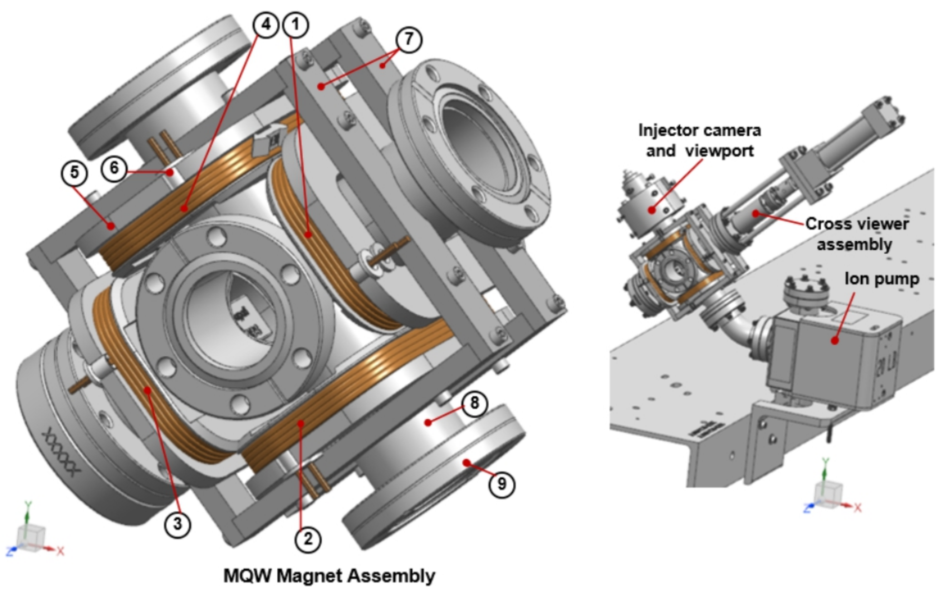

Figure 2: The MQW magnet mounted onto the stainless-steel CF six-way cross fitting [3]. The coils are oriented such that the lead wires point towards the exit side of the beam through the magnet assembly. Assuming that this assembly is viewed from the aforementioned side, then labels 1-4 denote respectively the MQW air-core racetrack coils QC1, QC2, QC3, and QC4. Label 5- coil bobbin, label 6- Rulon® bushing, label 7-magnet coil mounting assembly, and label 8-CF six-way cross-fitting and label 9- CF flange. The inset of the figure (right panel) shows the vacuum and diagnostic components attached to the six-way cross-fitting. +Z-axis point to the beam direction.

Table 1: The design parameters of the MQW quadrupole corrector magnet. See Figure 3-Figure 6 for detailed dimensions.

Part	Parameters	Unit	Design
Magnet wire	Material, Shape		Copper; Square with round corner
	Insulation		Polyimide (Kapton)
	Bare conductor size (equivalent AWG)		12
	Bare dimensions (maximum): width=thickness, corner radius	mm	2.077, 0.508
	Dimensions with insulation (maximum): width=thickness	mm	2.2047
Coil bobbin	Material		SS 304
	Inner gap: radial (horizontal), longitudinal (longitudinal)	mm	38.484, 85.427
	Thickness of the bobbin core	mm	2.5
	Thickness of the top flange, bottom flange	mm	6.35, 3.175
	Overall length, Overall height	mm	122.01, 19.39
	Thickness of kapton tape surrounding bobbin core	mm	0.508
	Thickness of pre-cut kapton spacer between the flat surface of the coil and top and bottom flanges of the bobbin	mm	0.508
Coil	Material		Copper
	Epoxy		AREMCO® 526 N
	Inner gap: radial (horizontal), longitudinal (longitudinal) of the coil	mm	44.5, 91.443
	Width (horizontal), and height (vertical) of the winding	mm	13.278, 8.849
	Overall length and overall width of the coil	mm	118, 71.057
	Inner corner radius	mm	10
	Total turn count (Number of layers, turns per layer) per coil		24 (6,4)
	Thickness of E-glass wrap on the outer surface of the coil (two layers of 0.1mm thick E-glass tape painted with epoxy)	mm	0.2
	Length of lead wires from the coil	m	1
	Estimated length of copper wire per coil (including lead wires)	m	~8.9
Bushing with flange	Material		Rulon
	Inside diameter, outside diameter of the bushing	mm	3.556, 6.198
	Height of the bushing, excluding the top flange	mm	6.477
	Outside diameter, thickness of the flange	mm	11.176, 1.397
Magnet Assembly*	Distance between the opposite pair of coils	mm	76
	Number of coils per magnet		4
	The overall dimensions of the MQW magnet mounted onto the six-way cross cube assembly	mm	123.14 (horizontal) 123.14 (vertical) 122 (longitudinal)
Note: Model number for QW coil bushing with flange- JL0091130-0223-02 *Refer to CAD model JL0091130-0226 for the coil mounting assembly details.			

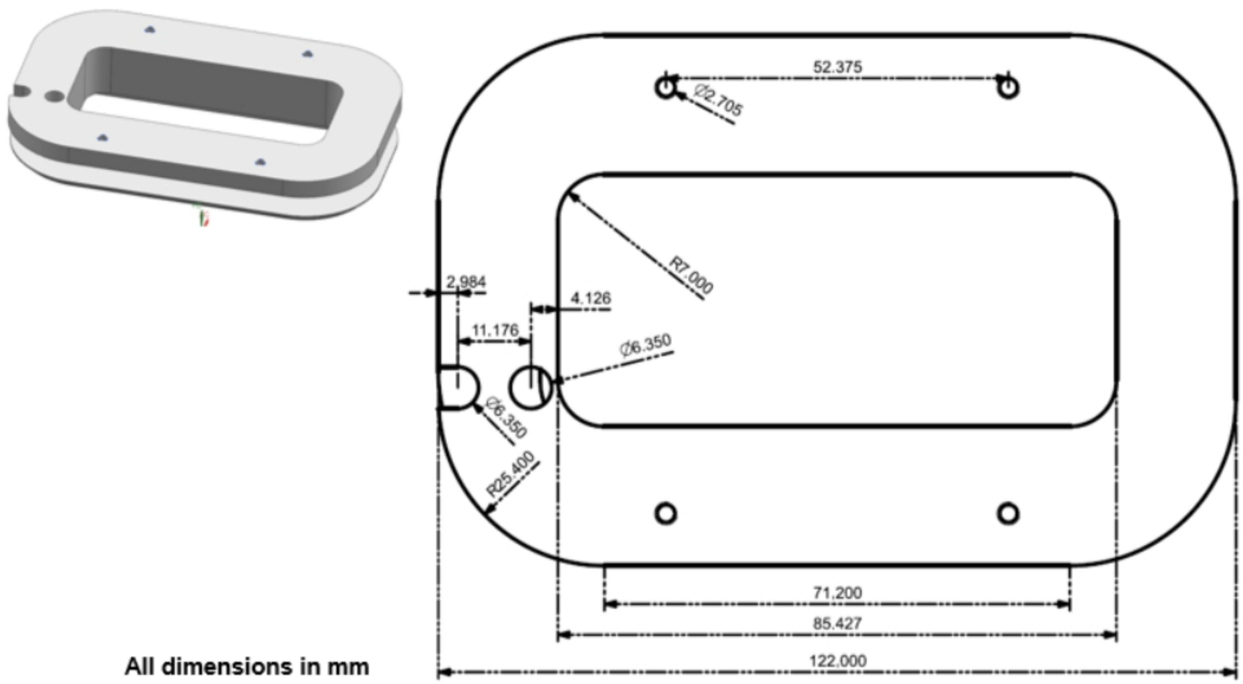

Figure 3: Top view of the design model and the detailed dimensions of the MQW coil bobbin.

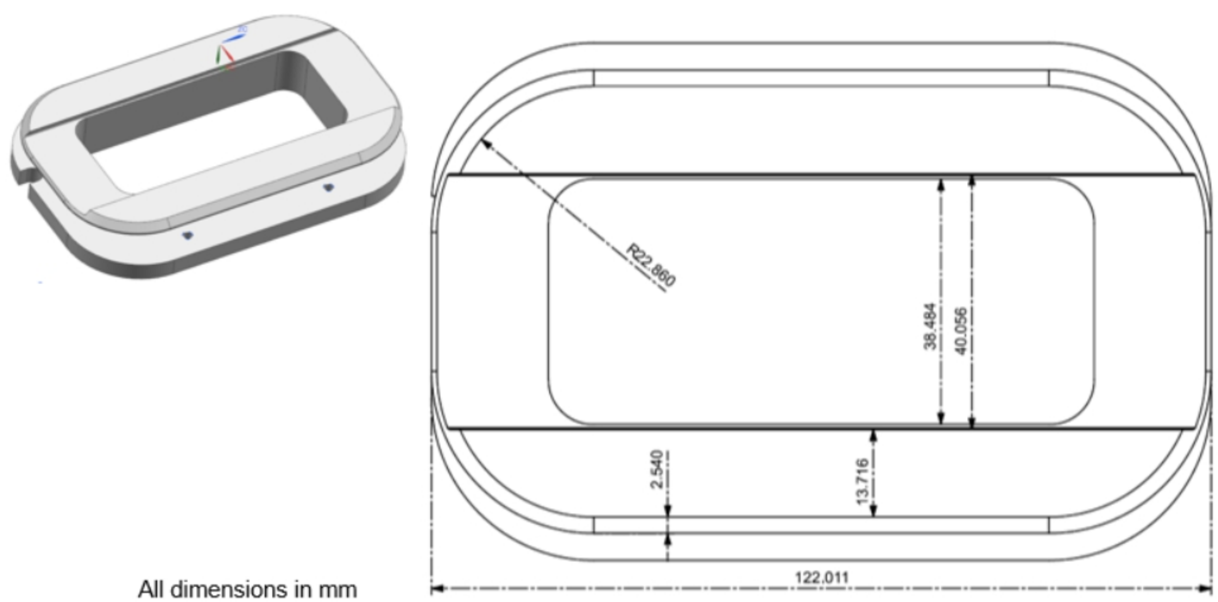

Figure 4: Bottom view of the design model and the detailed dimensions of the MQW coil bobbin.

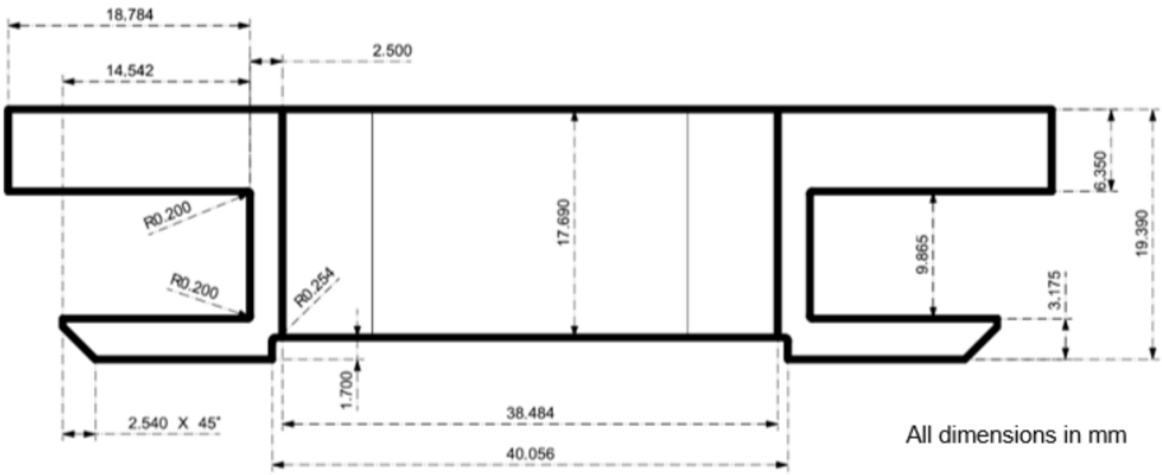

Figure 5: Transverse cross-sectional view of the model and the detailed dimensions of the MQW coil bobbin.

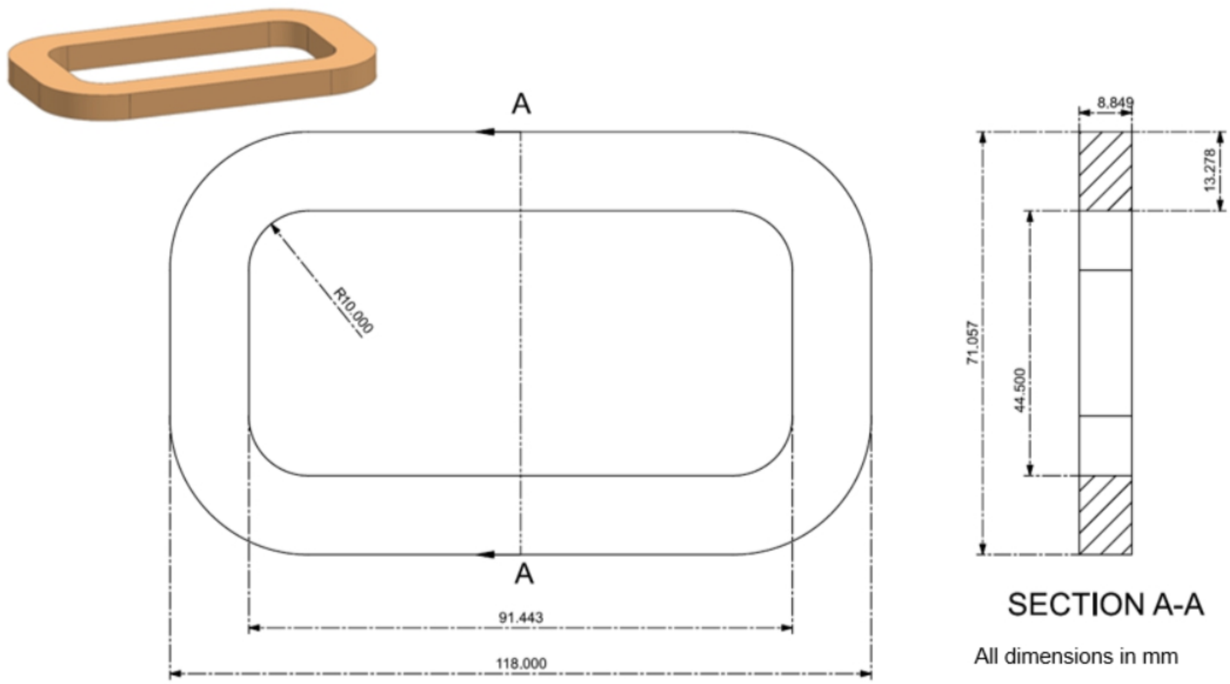

Figure 6:The top view and transverse cross-section of the model detailed dimensions of the MQW racetrack coil.

4.2 The coil design is optimized for the use of AWG12 square copper wire with round corners and with polyimide heavy film insulation. The coil manufacturing and magnet assembly requirements are given below.

4.2.1 All coils of a given lot shall use the magnet wire from the same production batch.

4.2.2 The racetrack coil shall be wet wound on the stainless-steel bobbin (label 5 in Figure 2) using a single, uninterrupted length of copper wire and AREMCO® 526 N ultra-high temperature epoxy.

4.2.3 Kapton film provides electrical insulation between the bobbin and the coil: (a) the outside surface of the bobbin core shall be wrapped with two layers of 0.254 mm thick Kapton tape; (b) Similarly, 0.508 mm thick pre-cut Kapton spacer shall be used between the flat surfaces of the coil and the top and bottom flanges of the bobbin.

4.2.4 The winding shall begin in the clockwise direction from the top flange side of the bobbin and complete also at the same side of the bobbin flange to simplify lead wire routing for the electrical termination of the magnet assembly.

4.2.5 Each coil shall contain 24 turns distributed over six consecutive layers (Figure 7). There are four turns per layer. Grooves shall be added to the outside surface of the bobbin core to regulate the winding pattern of the coils. All coils in a given lot shall have identical turn counts.

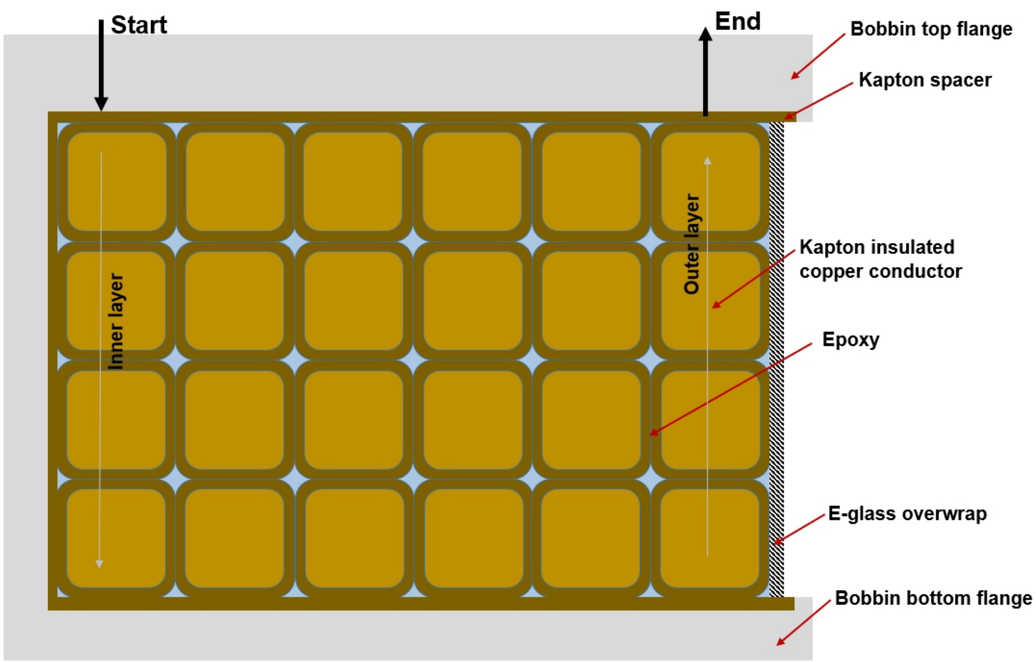

Figure 7: The conductor layout in the QW coil winding.

4.2.6 The leads shall be 36 inches (0.92 m) long.

4.2.7 G-10 shim shall be used to fill the void and to allow a smooth transition of the wire between the neighboring layers of the winding pack.

4.2.8 The lead wires shall exit through the openings (diameter=6.56 mm) made on the top flange of the bobbin (See Figure 8). The openings shall contain Rulon bushing (Table 1) to provide an insulating barrier between the lead wire and the top flange and strain relief for the section of the lead wire close to the winding pack.

4.2.9 The labels for the lead wires and the coil winding direction indicated by an arrow (see Figure 8) shall be engraved on the top flange of the bobbin.

Approved: 08/11/2021; E-Sign ID: 445894; Signed By: Reviewer 1: J. Grames; Reviewer 2: J. Grames; DCG Quality Check: T.

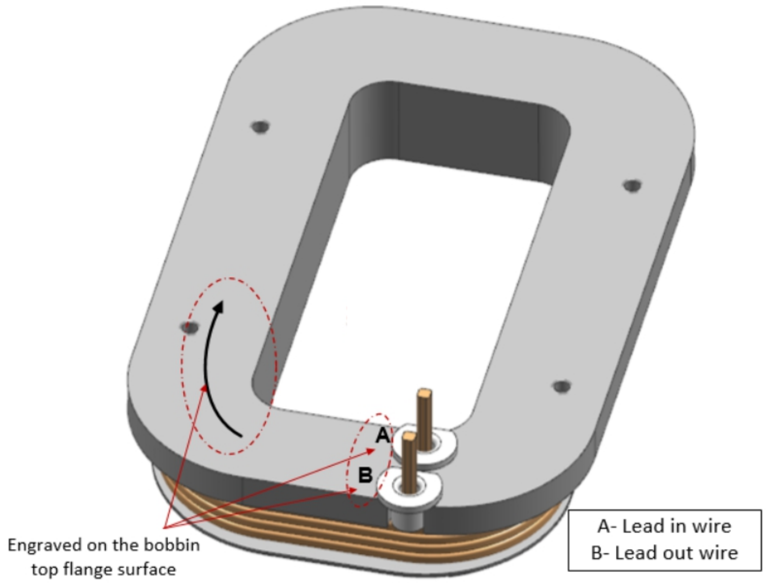

Figure 8: The lead wire labeling scheme for the MQW coils. The black arrow indicates the direction of the conductor winding. The labels A and B are engraved on the top flange of the bobbin points at the lead-in and lead-out wires from the winding pack.

4.2.10 The outer surface of the winding pack shall be wrapped under tension with two layers of 0.1 mm thick E-glass cloth and painted subsequently with AREMCO® 526 N epoxy. The same epoxy shall be used to secure the Rulon bushing in place on the top flange of the bobbin and to fill space between the lead wire and the inside surface of the bushing. The excess epoxy shall be carefully removed before curing the coils.

4.2.11 The finished wet coil shall be baked in the oven at 93.3°C for 3 hours followed by 2 hours at 162.8°C.

4.2.12 The lead wires shall be protected against damage during the coil manufacturing process.

4.2.13 The bottom-most section of the lead wire shall be reinforced further with 3M 361 glass cloth tape with silicone adhesive. Subsequently, the lead wire shall be dressed with a fiberglass fabric sleeve.

4.2.14 The lead wires shall be trimmed as needed, and terminal lugs shall be crimped onto the lead end.

4.3 The magnet assembly steps are as follows.

4.3.1 The MQW coils shall be installed onto the respective tubing of the 6-way cross-fitting. Additional mechanical supports shall be used to protect the coils and lead wires against damage due to handling.

4.3.2 The coil position shall be adjusted to facilitate the welding of the CF flange to the cross-fitting. The coils shall be protected from heat and weld spatter.

4.3.3 The mounting bars shall be attached subsequently to the outside surface of the top flange of the coil bobbin. Additional support blocks shall be used to hold the remaining coils in place.

4.3.4 The coils shall be repositioned to align the four mounting bars in the form of a rectangular frame and then fasten the adjacent units using an 18-8 stainless-steel socket head screw.

4.3.5 The inside surface of the CF flanges shall be protected during the assembly with a suitable plastic cap to prevent damages to the knife edge.

5 As-Built Coil Parameters

J Lab awarded the MQW coil manufacturing contract to Technicoil Inc. USA. They procured the copper wire from Rea Magnet Wire Company Inc., USA, and manufactured bobbin and the coils as per the drawings (Table 2) and manufacturing specification (see section 4) provided by JLab. The as-built coils have 23 turns spanning 6 layers of winding.

Table 2: The list of CAD drawings (PDF) based on the design parameters of the new MQW magnet.

	Reference number	Description
1	JL0091130-0223-01	MQW coil bobbin
2	JL0091130-0223-02	MQW bushing
3	JL0091130-0223-04	MQW coil
4	JL0091130-0226-01	MQW mount bar tapped
5	JL0091130-0226-02	MQW mount bar

We acquired thirty-two coils, sixteen from this lot have been used to assemble the four MQW type magnets for the Wien girder assembly. Table 3 shows the actual dimensions of the copper wire and the average dimensions of the production coils. The measured values of bobbin dimensions agree well with the original specification (Table 1) and are within the fabrication tolerance specified in the corresponding CAD drawing (item 1 in Table 2).

Table 3: The nominal dimensions of the magnet wire and the coils fabricated for the MQW magnet.

Parameter	Unit	Value
Magnet Wire (Supplier: Rea Magnet Wire Company Inc. USA)		
Bare wire conductor width (average value), height (average value)	mm	2.08, 2.08
Insulated wire diameter width (average value), height (average value)	mm	2.16, 2.16
MQW Coils (Manufacturer: Technicoil Inc. USA)		
Turn counts per coil		23
Overall length (average value)	mm	119.62
Overall width (including E-glass wrap) (average value)	mm	70.95
Width (horizontal) of the coil winding (average value)	mm	13.01
Height (vertical) of the coil winding (average value)	mm	8.68
Length of lead wire	m	0.92
Length of the copper wire per coil (including lead wires)	m	~8.4

6 Electrical Wiring Diagram

The MQW magnets are installed in the girder in such a manner that the lead wires of the respective coil assemblies remain on the side away from the CF end flanges of the adjacent horizontal or the vertical Wein filter assembly. Accordingly, the MQW1I03 and MQW1I05 magnet lead wires are positioned at the entrance side of the beam through the magnet. On the other hand, the MQW1I04 and MQW1I06 magnet leads are found at the exit side of the beam through the magnet (see the left panel of Figure 9).). The electrical wiring scheme of the coil pack is given in the same figure.

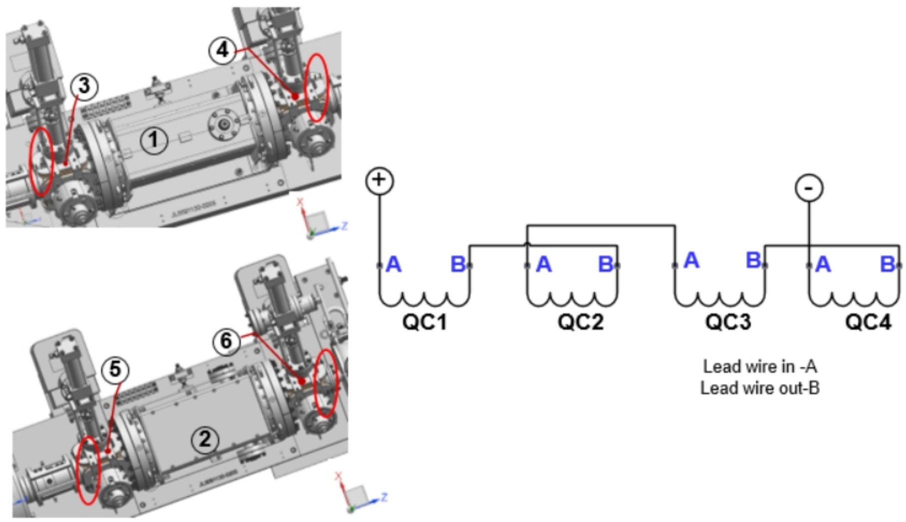

Figure 9: The electrical wiring diagram for the MQW coil assemblies. Figure 8 shows a closer view of the location of the lead wires from the coil.

7 Results and Discussion

7.1 Table 4 shows the magnetic performance parameters at the maximum integrated quadrupole field gradient of 100×10^{-4} T (100 Gauss) along the longitudinal axis of the magnet. As per the primary design specification (see the notes in the first row of Table 4), the MQW quadrupole magnet, with 24 turn counts per coil, needs to be energized at 7.15 A, whereas the performance validation studies indicate that the actual assembly with 23 turn counts per coil, requires 7.38 A to meet the same functional requirements.

7.2 The coils are designed with a sufficient safety margin (both operating current and temperature). For instance, the anticipated temperature of the coil at 10 A is $\leq$ 35°C. The MQW magnet assembly is energized using a 10 A trim card power supply.

7.3 The inner corners of the winding are subject to the highest field strength (Figure 10). For example, the production coil assembly sees a maximum of 9.34 mT at 7.38 A. The peak field in the actual coils in the MQW magnet increases linearly at a rate of 1.26 mT/A.

7.4 As presented in Figure 11 and Figure 12, the field errors of MST arise entirely from the first allowed higher-order harmonics, i.e. 12-pole component. Further, the peak strength of the 12-pole field component is almost three orders of magnitude smaller than the main quadrupole component for any given excitation current $\leq$ 10 A.

7.5 The overall strength of the quadrupole field of the production coil assembly at R_{GFR} increases linearly at a rate of 1.036×10^{-4} T/A (inset of Figure 12 (a)), whereas the corresponding 12- pole field component varies at a rate of 1.753 $\times 10^{-8}$ T/A (inset of Figure 12 (b)).

7.6 The integrated quadrupole field and integrated 12-pole field at R_{GFR} varies respectively at a rate of 10.164 × 10^{-6} T.m/A (see Figure 13 (a)) and 0.0175 10^{-6} T.m/A (see Figure 13 (b)). Similarly, the transfer function for the quadrupole integrated field gradient is 13.6 10^{-4} T/A as shown in the inset of Figure 13 (a). The effective magnetic length is 9.81 × 10^{-2} m (Table 4). The calculated value of the integrated quadrupole field uniformity in GFR is better than 99.99 %. Table 5 provides a tabular form of the quadrupole integrated field strength at R_{GFR} as well as the quadrupole integrated field gradient for coil excitation current up to 10 A These data will be used in the CEBAF machine control system.

Table 4:Performance parameters at the maximum operating conditions of the MQW magnet.

Parameter	Unit	Value	
ANSYS Maxwell case studies		**Based on the primary design model** *(See Table 1 for coil and bobbin model parameters)*	**Based on the performance validation model** *(See Table 3 for the production coil model parameters and* Table *1 for coil bobbin parameters)*
Reference radius (R_{GFR})	mm	7.5	7.5
Max. operating current of the coil (I_{max})	A	7.15	7.38
Operating current density in the copper wire	A/mm²	1.75	1.8
The maximum field strength in the coil pack	mT	9.384	9.339
Integrated quadrupole field strength along the longitudinal axis and at R_{GFR} $\left(\int_{z=-0.3m}^{z=+0.3m} B_{r,n=2}(R_{GFR}, z)\,.\,dz\right)$	T.m	7.50E-05	7.50E-05
Integrated quadrupole field gradient along the longitudinal axis	T	100E-04	100E-04
Effective magnetic length (L_{eff}) of the quadrupole magnet	m	9.75E-02	9.81E-02
Integrated strength along the longitudinal axis and at R_{GFR} of 12-pole field component $\left(\int_{z=-0.3m}^{z=+0.3m} B_{r,n^*=6}(R_{GFR}, z)\,.\,dz\right)$	T.m	7.46E-09	7.04E-09
Quadrupole integrated field quality at R_{GFR}	%	99.99	99.99
The magnetic stored energy at I_{max}	mJ	8.71	8.55
Total Inductance of the MQW magnet	µH	341	313.9
The resistance of the MQW coil at 20 °C.	mΩ	32.5	35.18
Cumulative strength of Lorentz force (F_{cum}) at I_{max}in the single racetrack coil	mN	24.6	24.1

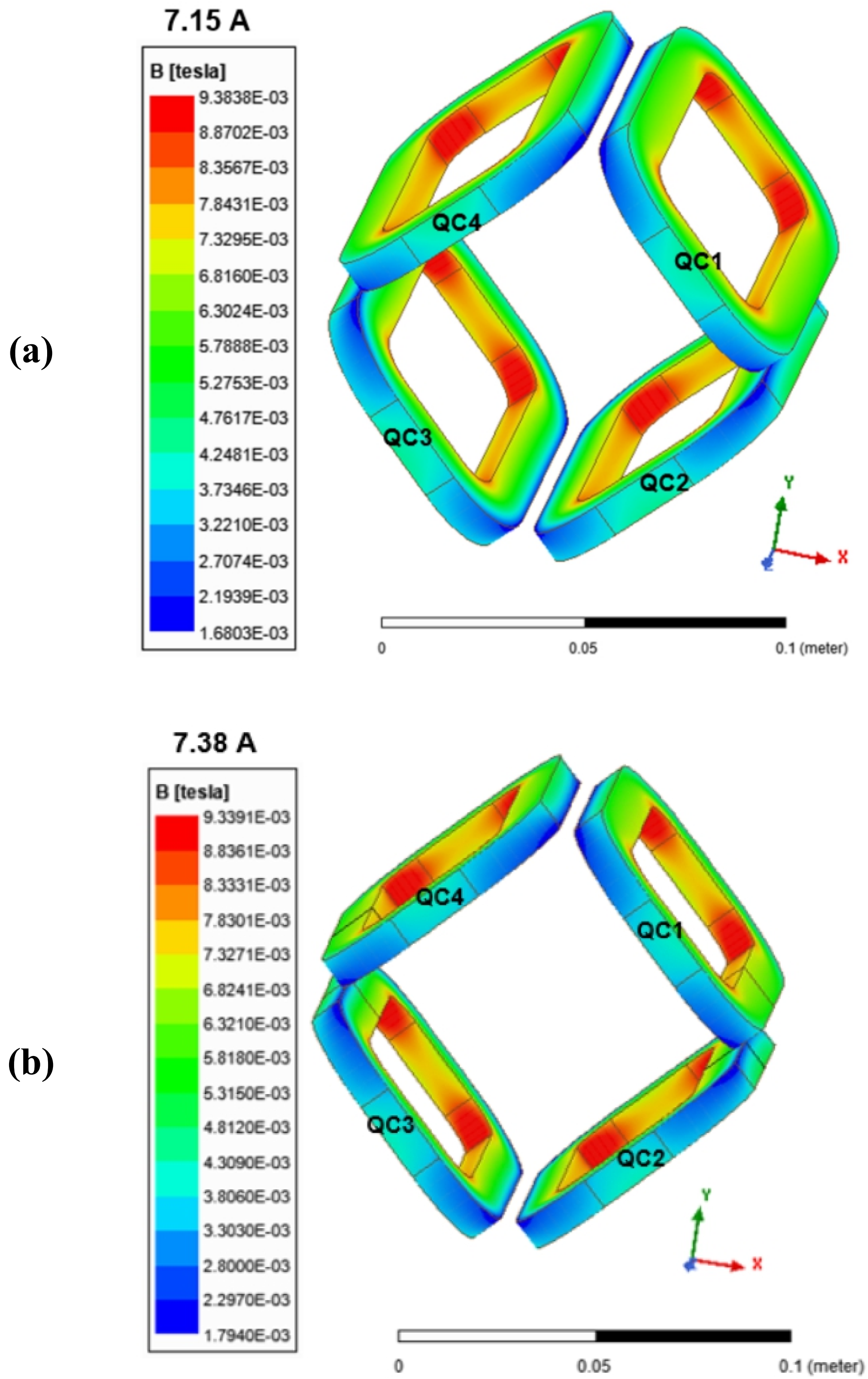

Figure 10: The magnetic field distribution at the maximum operating conditions of the MQW magnet: (a) at 7.15 A (see Table 1 for the primary design specification), and (b) at 7.38 A (see Table 3 for the nominal dimensions of the MQW production coils).

(a)

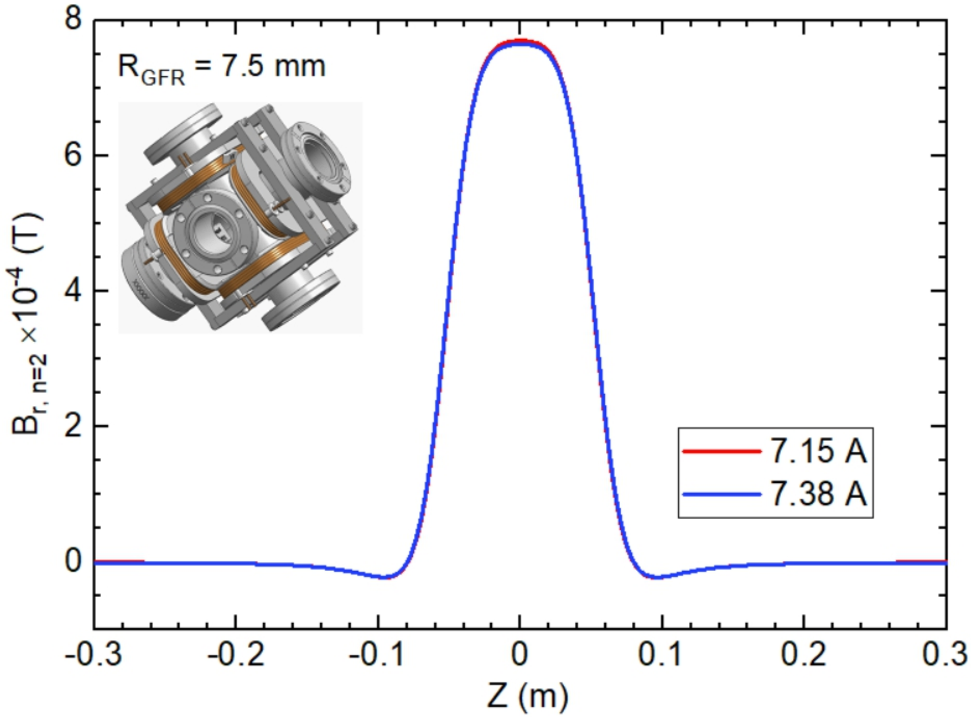

(b)

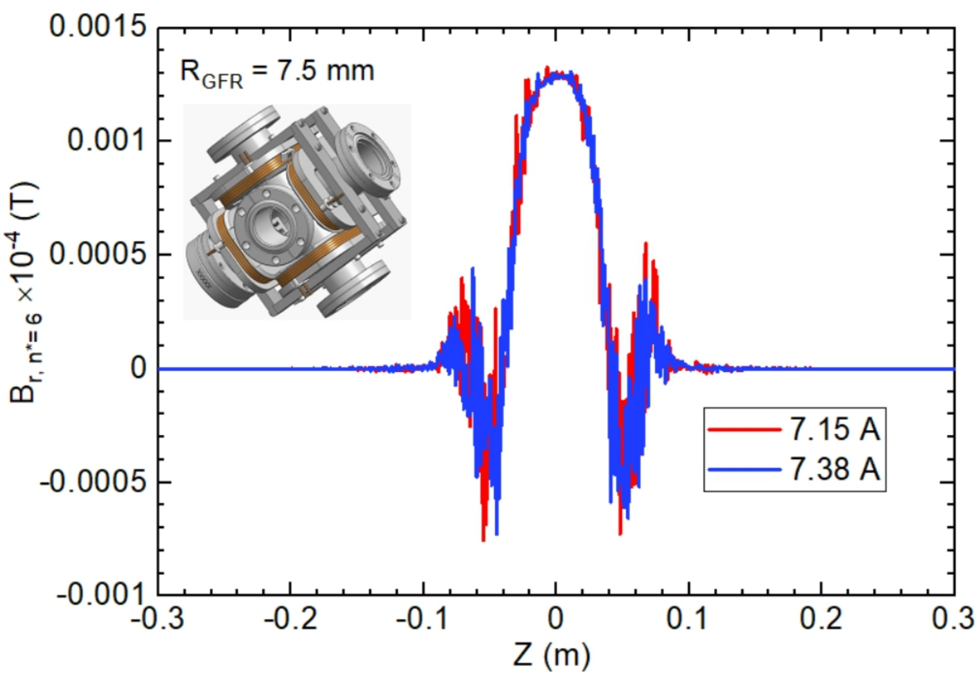

Figure 11:(a) The quadrupole field $(B_{r,n=2})$ and (b) 12-pole harmonic field $(B_{r,n^*=6})$ profile along the longitudinal direction (Z-axis) of the MQW magnet at 7.15 A (as per the primary design model parameters listed in Table 1**) and 7.38 A (model based on the as-built coil parameters given in Table 3). The reported values are at R_{GFR}= 7.5 mm.**

(a)

(b)

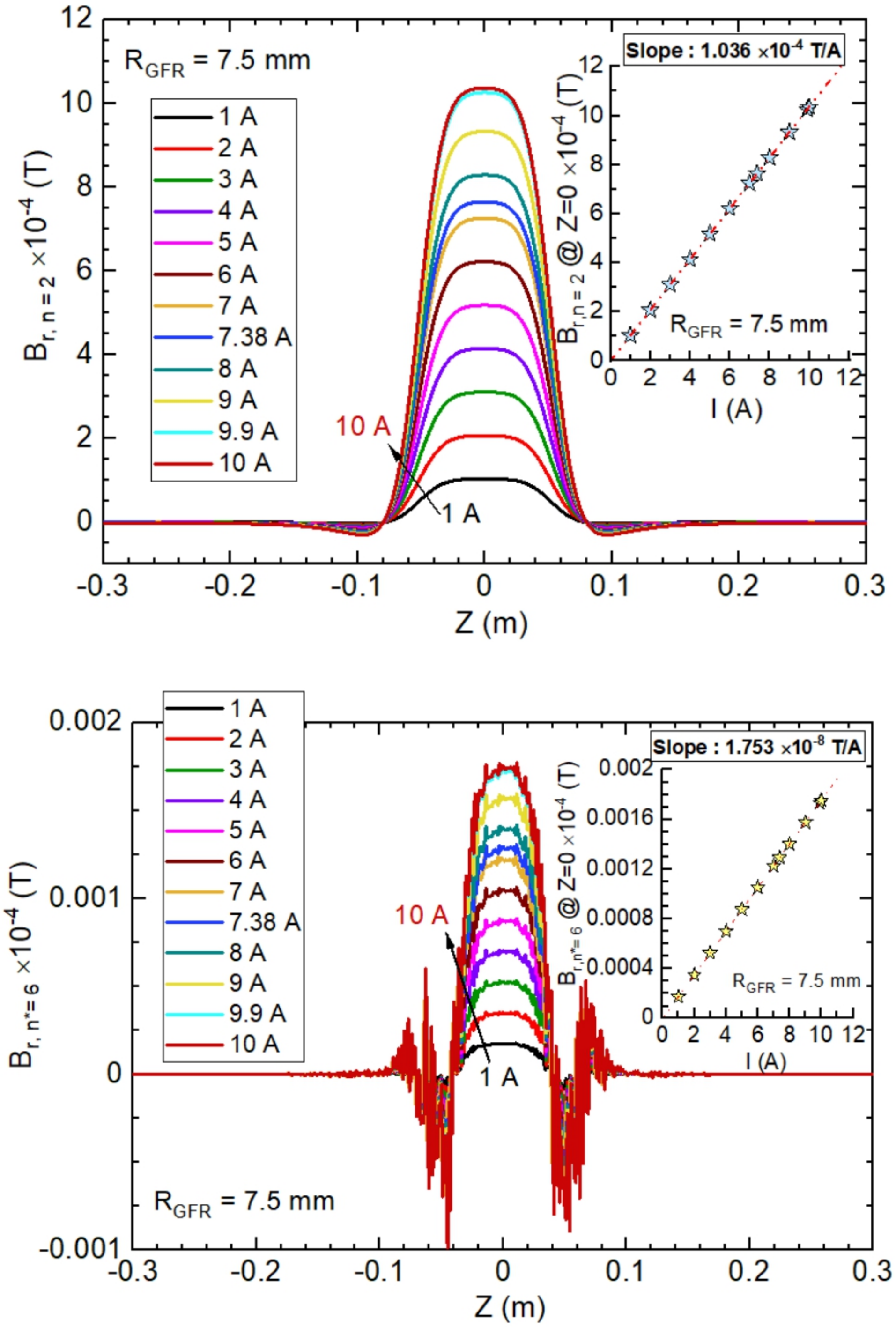

Figure 12: a) The quadrupole field $(B_{r,n=2})$ and (b) 12-pole harmonic field $(B_{r,n^*=6})$ profile along the longitudinal direction (Z-axis) of the MQW magnet for I ≤ 10 A. These data are obtained from the 3D EM simulation of the model based on the as-built coil parameters as shown in Table 3. The reported values are at R_{GFR} = 7.5 mm. The dotted lines in the inset figures represent the linear fit of the peak field values for I ≤ 10 A.

(a)

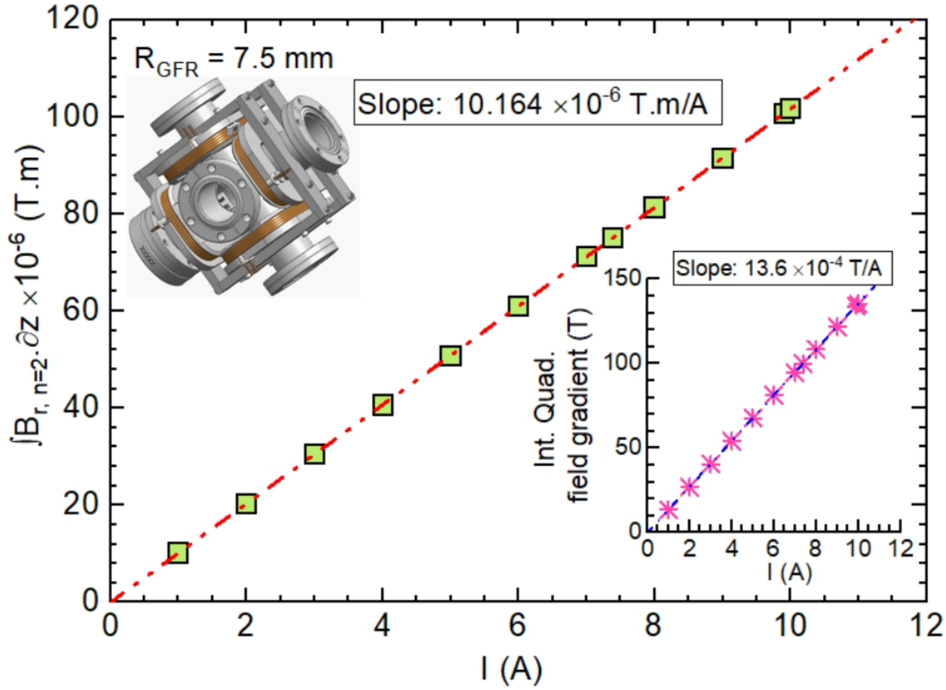

(b)

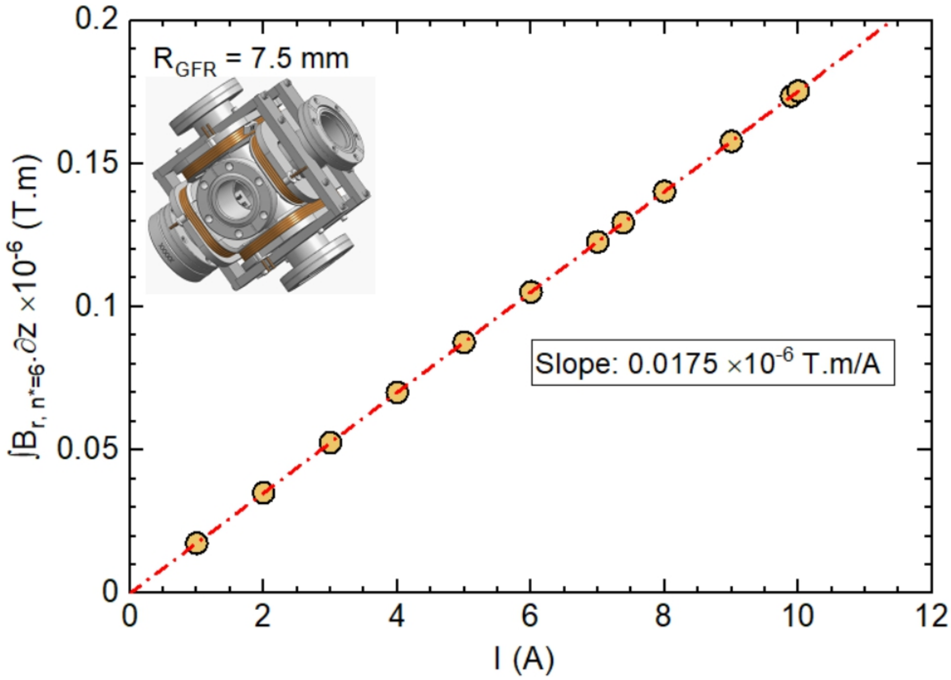

Figure 13: The solid symbols represent the integrated (a quadrupole field strength and (b) the 12-pole harmonic field strength at R_{GFR} = 7.5 mm and coil excitation current ≤ 10A of the MQW magnet. These data are obtained from the 3D EM simulation of the magnet model according to the as-built coil parameters given in Table 3. The dot-dash line represents the linear fit to the data plotted in the same figure. The inset of the top panel (a) shows the corresponding integrated quadrupole field gradient for the same range of the excitation current.

Table 5: Integrated quadrupole field strength at R_{GFR}=7.5 mm and integrated quadrupole field gradient at I ≤ 10 A (same as the data presented in Figure 12(a)) for the MQW magnet. The data is obtained from the 3D EM simulation of the as-built coil models. See Table 3 for the coil parameters.

Operating current (A)	Integrated quadrupole field strength at R_{GFR}=7.5 mm ×10^{-6} (T.m)	Integrated quadrupole field gradient ×10^{-4} (T)
0	0	0
1	10.164	13.55
2	20.327	27.1
3	30.491	40.65
4	40.654	54.21
5	50.818	67.76
6	60.981	81.31
7	71.145	94.86
7.38	75.007	100.01
8	81.308	108.41
9	91.472	121.96
9.9	100.619	134.16
10	101.635	135.51

Table 6: The inductance matrix of the MQW magnet. The data is obtained from the 3D EM simulation of the as-built coil models. See Table 3 for the coil parameters.

MQW assembly (Unit: H)				
	QC1	QC2	QC3	QC4
QC1	6.56E-05	7.89E-06	-2.88E-06	7.89E-06
QC2	7.89E-06	6.56E-05	7.89E-06	-2.88E-06
QC3	-2.88E-06	7.89E-06	6.56E-05	7.89E-06
QC4	7.89E-06	-2.88E-06	7.89E-06	6.56E-05

7.7 The inner corners of the winding are subject to the highest field strength (Figure 10). For example, the production coil assembly sees a maximum of 9.34 mT at 7.38 A. The peak field in the actual coils in the MQW magnet increases linearly at a rate of 1.26 mT/A.

7.8 As presented in Figure 11 and Figure 12, the field errors of MST arise entirely from the first allowed higher-order harmonics, i.e. 12-pole component. Further, the peak strength of the 12-pole field component is almost three orders of magnitude smaller than the main quadrupole component for any given excitation current ≤ 10 A.

7.9 The overall strength of the quadrupole field of the production coil assembly at R_{GFR} increases linearly at a rate of 1.036×10^{-4} T/A (inset of Figure 12 (a)), whereas the corresponding 12- pole field component varies at a rate of 1.753 $\times 10^{-8}$ T/A (inset of Figure 12 (b)).

7.10 The integrated quadrupole field and integrated 12-pole field at R_{GFR} varies respectively at a rate of 10.164 $\times 10^{-6}$ T.m/A (see Figure 13 (a)) and 0.0175 10^{-6} T.m/A (see Figure 13 (b)). Similarly, the transfer function for the quadrupole integrated field gradient is 13.6 10^{-4} T/A as shown in the inset of Figure 13 (a). The effective magnetic length is 9.81 $\times 10^{-2}$ m (Table 4). The calculated value of the integrated quadrupole field uniformity in GFR is better than 99.99 %. Table 5 provides a tabular form of the quadrupole integrated field strength at R_{GFR} as well as the quadrupole integrated field gradient for coil excitation current up to 10 A These data will be used in the CEBAF machine control system.

7.11 The inductance matrix of the MQW production coil assembly is given in Table 6. The number in diagonal from the upper-left to the lower-left corners represents the self-inductances of the coils (65.6 µH) in the MQW assembly, whereas the non-diagonal numbers signify the mutual inductances between those coils. The total inductance of the magnet assembly is 313.9 µH (Table 4).

7.12 The estimated value of the resistance of the MQW coil at 20°C is 35.18 mΩ (Table 4). Therefore, the anticipated value of the resistance of the MQW coil magnet (including the 0.92 m long lead wires) at 20°C is 140.7 mΩ.

7.13 The net force of the MQW assembly is dominated by the horizontal (F_x) and vertical (F_y) field components. The net value of the longitudinal (F_z) force component is practically negligible. Both F_x and vertical F_y are equal in magnitude and compressive in nature. The net cumulative force at 7.38 A is 24.1 mN. The coil-bobbin assemblage in the quadrupole configuration is secured in place by using the coil mounting assembly frame (label 7 in Figure 2). The original concept of the coil mounting frame developed from the detailed EM-structural design and analysis was not implemented in the actual assembly. Since the mounting components were already fabricated, a decision has been made to them in the magnet assembly. To minimize the potential magnetic alignment errors resulting from coil mounting frame assembly, shims (rectangular in shape with dimensions: 70 mm (length) × 15mm (width) × 0.1778 mm (thickness); material: SS 304)) shall be added to the inside surface of the coil-bobbin assemblage.

8 Test Plan

The magnet measurement facility presently has the test set up to perform the magnetic profile measurements using only a uni-axial hall probe. The magnetic field measurement plan is provided in section #8.3. These data will be compared against the EM simulation results of the magnet assembly model based on the production coil parameters (Figure 14). Multipole field analysis of the EM simulation data will be used to extract the relevant physics parameters for the magnet system and to provide data to the CEBAF machine control system.

8.1 Quality Assurance tests

8.1.1 Perform the visual inspection and record the observations.

8.1.2 Record the wire dimensions at three pre-selected locations of the two lead wires and note down the average value.

8.1.3 Record the overall length and overall width of the coil

8.1.4 Record the room temperature resistance of the coil (note down the ambient conditions)

8.1.5 Record the coil inductance at 20 Hz,60 Hz, and 100 Hz.

8.1.6 Hipot and surge test at 1000 V; Record the leakage current (qualification criterion: leakage current shall be ≤ 5 μA).

8.1.7 Record the temperature evolution of one representative coil energized at 7.5 A and 10 A. Monitor the temperature readings at least for four hours.

8.2 Assemble one MQW magnet on the dummy 6-way cross assembly. Dress the lead wires. Complete the electrical wiring connections according to Figure 9 in this document.

8.3 Record the room temperature resistance and inductance at 60 Hz of the magnet.

8.4 Magnetic field measurements of the MQW assembly

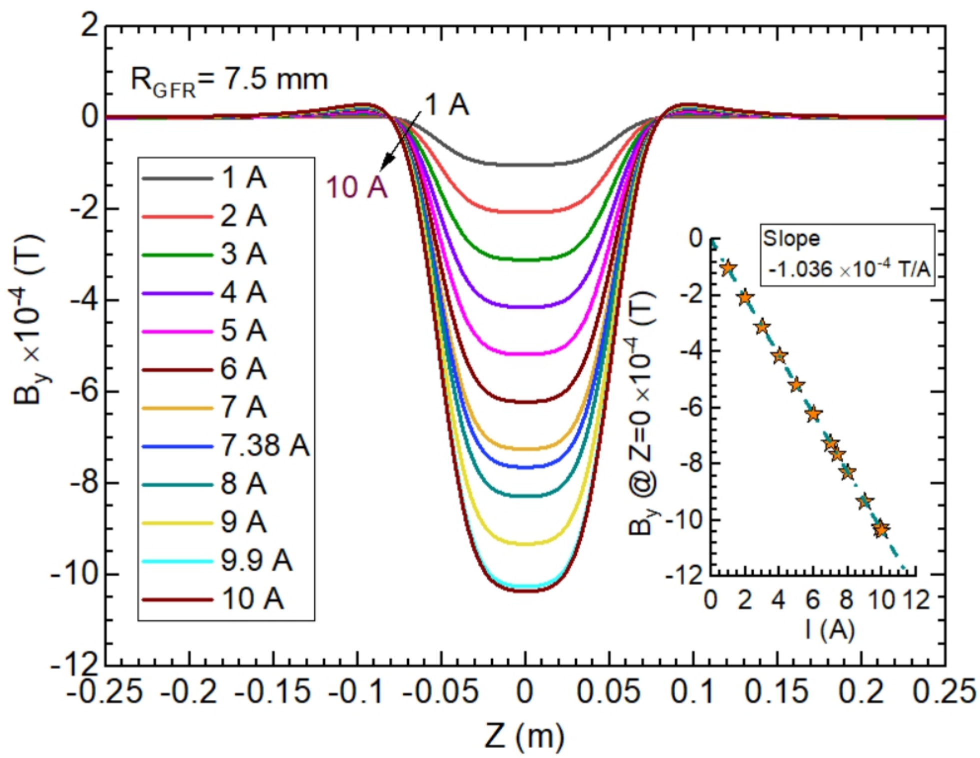

Figure 14: The vertical field (B_y) profile over Z = ±0.25 m from the magnet center (X = 0, Y = 0, Z = 0) of the MQW for coil excitation currents ≤ 10A and at R_{GFR} of 7.5 mm. This data is obtained from the EM simulation of the magnet model using the production coil parameters listed in Table 3. Refer to for the electrical wiring diagram. Table 7 provides the value of the integrated strength of the vertical field component over the same Z range and for I≤ +10 A.

8.3.1 Measure vertical field (B_y) versus Z at X values indicated below and at I = 0 A with coils and dummy 6-way cross assembly (background measurements).

8.3.1.1 Z range: ±0.25 m from the magnet center.

8.3.1.2 Z step: at 10 mm interval from Z=-0.25 m to -0.20 m; at 2 mm interval from Z = - 0.2 m to +0.2 m; at 10 mm interval from Z=0.20 m to 0.25 m.

8.3.1.3 X= -10 mm, -7.5 mm, -5 mm, +5 mm, +7.5 mm, +10 mm (X denotes the horizontal distance from the magnet center).

8.3.2 Measure $B_y\ (Z)$ at X values indicated below and at I=8 A

8.3.2.1 Z range: same as #8.3.1.1

8.3.2.2 Z step: same as #8.3.1.2

8.3.2.3 X= same as #8.3.1.3.

8.3.3 Repeat the background measurement at X= +7.5 mm and Z range specified above

8.3.4 Measure $B_y\ (Z)$ at X=+7.5 mm and I=±9 A.

8.3.4.1 Z range: same as #8.3.1.1.

8.3.4.2 Z step: same as #8.3.1.2.

8.3.5 Repeat the background measurement at X= +7.5 mm and Z range specified above

Table 7: Integrated strength of vertical field component at R_{GFR}= 7.5 mm and I ≤ 10 A for the MQW magnet. Figure 14 shows the corresponding $B_y(Z)$ profile from the 3D EM simulation of the as-built coil models. See Table 3 for the coil parameters.

Operating current (A)	$\int_{-0.25m}^{+0.25m} B_y\,(R_{GFR}=7.5mm, z\,).\partial z$ ×10^{-6} (T.m)
0	0
1	-10.174
2	-20.348
3	-30.522
4	-40.696
5	-50.870
6	-61.044
7	-71.219
7.38	-75.085
8	-81.393
9	-91.567
9.9	-100.723
10	-101.741

9 Summary

The electromagnetic-mechanical design analysis and performance validation studies suggest that the new MQW quadrupole corrector magnet for the 200 keV injector beamline meets the overall performance requirements. The MQW magnet needs to be energized at 7.38 A to achieve the highest quadrupole integrated field gradient of 0.01 T (100 Gauss). The coils are designed with a sufficient safety margin. The magnet will require a 10 A power supply. The magnetic analysis results indicate that the field errors are due to the first allowed harmonics, the 12-pole field component. The integrated field strength of the 12-pole field component is approximately four orders of magnitude smaller than that of the main quadrupole field component. The integrated field homogeneity in the good field region with a radius of 7.5 mm is better than 99.99 %. The coil temperature at the maximum operating current (10 A) is expected to stay below 35 °C during the continuous operation in the beamline. All components used in the coils and magnet assembly can withstand a maximum of 200 °C to comply with the bake-out procedure for the beamline vacuum components.

10 References

[1] J Lab Drawing ACC0002845-0001: ACC Machine configuration- Beam transport injector.
[2] J Lab NX CAD 3D Model JL0091130-0202: Wein filter girder assembly.
[3] J Lab NX CAD 3D Model JL0091130-0222: MQW cross assembly